Differential expression of oxidation-specific epitopes and apolipoprotein(a) in progressing and ruptured human coronary and carotid atherosclerotic lesions

Rogier A. van Dijk,* Frank Kolodgie,* Amir Ravandi,† Gregor Leibundgut,† Patrick P. Hu,† Anand Prasad,† Ehtisham Mahmud,† Edward Dennis,§, Linda K. Curtiss,†† Joseph L. Witztum,† Bruce A. Wasserman,§§ Fumiyuki Otsuka,* Renu Virmani,* and Sotirios Tsimikas[1,†]**

CVPath Institute,* Gaithersburg, MD; Departments of Medicine,† Pharmacology,§ and Chemistry and Biochemistry,** University of California at San Diego, La Jolla, CA; Scripps Research Institute,†† La Jolla, CA; and Russell H. Morgan Department of Radiology and Radiological Sciences,§§ Johns Hopkins Hospital, Baltimore, MD

Abstract The relationships between oxidation-specific epitopes (OSE) and lipoprotein (a) [Lp(a)] and progressive atherosclerosis and plaque rupture have not been determined. Coronary artery sections from sudden death victims and carotid endarterectomy specimens were immunostained for apoB-100, oxidized phospholipids (OxPL), apo(a), malondialdehyde-lysine (MDA), and MDA-related epitopes detected by antibody IK17 and macrophage markers. The presence of OxPL captured in carotid and saphenous vein graft distal protection devices was determined with LC-MS/MS. In coronary arteries, OSE and apo(a) were absent in normal coronary arteries and minimally present in early lesions. As lesions progressed, apoB and MDA epitopes did not increase, whereas macrophage, apo(a), OxPL, and IK17 epitopes increased proportionally, but they differed according to plaque type and plaque components. Apo(a) epitopes were present throughout early and late lesions, especially in macrophages and the necrotic core. IK17 and OxPL epitopes were strongest in late lesions in macrophage-rich areas, lipid pools, and the necrotic core, and they were most specifically associated with unstable and ruptured plaques. Specific OxPL were present in distal protection devices. Human atherosclerotic lesions manifest a differential expression of OSEs and apo(a) as they progress, rupture, and become clinically symptomatic. These findings provide a rationale for targeting OSE for biotheranostic applications in humans.—van Dijk, R. A., F. Kolodgie, A. Ravandi, G. Leibundgut, P. P. Hu, A. Prasad, E. Mahmud, E. Dennis, L. K. Curtiss, J. L. Witztum, B. A.Wasserman, F. Otsuka, R. Virmani, and S. Tsimikas. **Differential expression of oxidation-specific epitopes and apolipoprotein(a) in progressing and ruptured human coronary and carotid atherosclerotic lesions. *J. Lipid Res.* 2012.** 53: **2773–2790.**

Oxidative pathways in the subendothelial space activate pro-inflammatory, immunogenic, and atherogenic processes, resulting in endothelial dysfunction, plaque growth and destabilization, platelet activation, and thrombosis, ultimately leading to clinical events (1). A variety of oxidation-specific epitopes (OSE) are generated during oxidative modification of plaque components. These epitopes are not only expressed on modified lipoproteins but also on apoptotic cells and proteins in the extracellular matrix of atherosclerotic vessels (2).

Extensive experimental data exists defining the role of oxidation in both progression and regression of atherosclerosis. Atherosclerotic lesions of hypercholesterolemic animal models, which represent primarily early and intermediate stage atherosclerosis, contain significant amounts of OSE, often in proportion to plaque burden. OSE in the vessel wall of atherosclerotic animals can also be imaged with nuclear and magnetic resonance techniques using murine and human oxidation-specific antibodies, such as MDA2, E06, and IK17 (3–5). Dietary interventions in hypercholesterolemic animals that promote regression result in more rapid removal of OSE than apoB, which occurs prior to plaques diminishing significantly in size, and is associated with markers of plaque stabilization, such

This work was supported by the CVPath Institute, Gaithersburg, MD, the Fondation Leducq, LIPID MAPS National Institutes of Health Grant 5 U54 GM-069338, and National Institutes of Health Grants HL-086559 and HL-088093. The LC-MS/MS work was supported by the National Institute of General Medical Sciences Large-Scale Collaborative "Glue" Grant U54 GM-069338. The contents are solely the responsibility of the authors and do not necessarily represent the official views of the National Institutes of Health. Drs. Tsimikas and Witztum are co-inventors of patents, owned by the University of California, on the potential clinical use of oxidation-specific antibodies. Drs. Tsimikas and Witztum are consultants to ISIS and Regulus, and they have equity interest in Atherotope.

Manuscript received 27 July 2012 and in revised form 10 September 2012.

Published, JLR Papers in Press, September 11, 2012
DOI 10.1194/jlr.P030890

Abbreviations: AIT, adaptive intimal thickening; apo(a), apolipoprotein (a); EFA, early fibroatheroma, H and E, hematoxylin and eosin; IX, intimal xanthoma; LFA, late fibroatheroma, Lp(a), lipoprotein (a); MDA, malondialdehyde-lysine; OSE, oxidation-specific epitope; OxPL, oxidized phospholipid; PIT, pathologic intimal thickening; PR, plaque rupture; SMC, smooth muscle cell; SVG, saphenous vein graft; TCFA, thin cap fibroatheroma.

[1]To whom correspondence should be addressed.
e-mail: stsimikas@ucsd.edu

as increased collagen and smooth muscle cell (SMC) expression, and a decrease in reactive oxygen species and macrophages (6–8).

Despite this wealth of animal data on the relationship of OSE and atherosclerosis, relatively little is known about their relationship to clinically relevant advanced, unstable, or ruptured plaques. Furthermore, a systematic analysis of the presence of OSE in human lesions has not been performed to date. Therefore, the purpose of this study was to determine the presence and relative distribution of well-characterized OSE in various stages of human atherosclerotic lesions, including native coronary lesions, carotid endarterectomy samples, and material from carotid and saphenous vein graft (SVG) embolic protection filters. Such knowledge may have significant clinical implications with the emergence in the clinical and translational arenas of oxidative biomarkers, molecular imaging, and therapeutic approaches, including immune modulation and vaccine approaches targeting these moieties (9–12), broadly characterized as "biotheranostic" (biomarker, therapeutic, diagnostic imaging) applications.

METHODS

Human atherosclerotic lesions

Hearts of patients who had died suddenly with coronary artery disease (CAD) were obtained as previously described (13). Cases were identified prospectively by the presence and type of CAD and included nonatherosclerotic intimal lesions, pathologic intimal thickening, early and late fibroatheroma, thin cap fibroatheroma (TCFA) and plaque rupture. Eighty-nine representative lesions from 25 consecutive patients (22 men and 3 women, age at death 47 ± 13) were selected prior to staining.

To rule out postmortem oxidation occurring prior to heart harvesting, we also evaluated carotid endarterectomy specimens (n = 13) from symptomatic patients undergoing clinically indicated procedures. The specimens were removed en bloc and immediately fixed in formalin. Additionally, we evaluated material derived from distal protection devices (n = 10) obtained during percutaneous intervention of stenotic internal carotid arteries and coronary SVGs. The entire filter material was immediately placed in ice-cold phosphate buffered solution of EDTA/BHT (100 μM / 20 μM), and then rapidly lipid extracted and stored at −80°C for analyses as described below.

To further rule out postmortem effects, we additionally evaluated five carotid endarterectomy specimens under various handling conditions as follows: each specimen was manually cut into three equal sections and stored at room temperature for 24 h in PBS (phosphate buffered saline), on ice for 24 h in PBS, or on ice in EDTA/BHT for 24 h, respectively. Each of the specimens was then paraffin embedded, and sections were placed on glass slides and immunostained as above.

Histological preparation

Formalin-fixed, paraffin-embedded coronary segments were cut into 5 μm thick sections, mounted on charged slides, and stained with hematoxylin and eosin (H and E) and the modified Movat pentachrome method as previously described (14).

Histological classification of lesions

Plaque components. In a single section, there may be several plaque components, independent of dominant plaque type. Those lesions that were prone to lipid accumulation, either intracellular or extracellular, were identified. Foam cell lesions were defined as areas of macrophages in the presence or absence of significant extracellular lipid (intimal xanthoma) (15). Lipid pools within pathologic intimal thickening (PIT) consisted of a proteoglycan-rich matrix with trapped lipid and absence of fibrin and hemorrhage in the deeper intima. These pools were often surrounded by macrophage foam cell or SMC-rich areas toward the lumen. Necrotic core denoted focal areas of necrotic debris with presence of apoptotic macrophage debris, prominent cholesterol crystals, and presence of fibrin with partial or complete loss of proteoglycan matrix (15). The presence of macrophages within the fibrous cap or shoulder region denoted cases of early and late fibroatheroma, thin fibrous cap atheroma, and ruptured plaques.

Plaque types. The dominant plaque type per coronary artery section was defined as adaptive intimal thickening (AIT, n = 7); intimal xanthoma (IX, n = 8); PIT (n = 11); early fibroatheroma (EFA, n = 25); late fibroatheroma (LFA, n = 17); thin-cap fibroatheroma (TCFA, n = 13); and acute plaque rupture (PR, n = 8). Lesions were classified according to a modification of the current American Heart Association recommendations (16). The distinction between early and late fibroatheroma was made as previously defined (16), namely, the complete loss of matrix and extensive cellular breakdown defined late fibroatheromas (17).

Antibodies

Five unique monoclonal antibodies were used in this study to assess the presence of apolipoprotein B-100, OSE, and apo(a). MB47 is an IgG murine monoclonal antibody that binds near the LDL-receptor domain of human apoB-100 (18). MB47 binds to all apoB-containing lipoproteins equally, and it also binds to fragments of apoB-100 on OxLDL if it is minimally to even extensively modified during oxidation by exposure to copper in vitro. E06 is a natural IgM murine monoclonal antibody cloned from apoE$^{-/-}$ mice that binds the PC headgroup of oxidized phospholipids (OxPL) and thus recognizes this whether the OxPL is free or covalently bound to proteins. Covalent binding of OxPL occurs via the reactive oxidized moieties, such as aldehydes, generated on the sn2 side chains when the phospholipids are oxidized. The PC is preserved in this setting and is the moiety recognized by E06. E06 recognizes a variety of OxPL with varying sn2 chain lengths terminated by aldehydes, such as 5, 6, and even 9 carbon lengths. It would not recognize oxovaleryl bound to protein unless it was present as the sn2 side chain of an OxPL (19, 20). MDA2 binds to malondialdehyde (MDA) adducts with lysine residues of proteins, in which MDA acts as a hapten on a protein carrier. It thus recognizes a wide variety of MDA-modified proteins (21). IK17 is a fully human Fab fragment generated with phage display library technology that also binds to MDA adducts with lysine, but it appears to be more specific for MDA-modified LDL, as it does not bind to MDA-modified BSA or polylysine (22).The chemistry of MDA modification is complex; we believe IK17 detects a more complex MDA adduct, although we have not definitely defined it. Uniquely, IK17 also binds to OxLDL, whereas MDA2 does not. Thus its epitope appears to be an MDA adduct that is present on both MDA-LDL and OxLDL. It does not bind OxPL. LPA4 is a murine monoclonal IgG antibody binding the sequence TRNYCRNPDAEIRP on apolipoprotein(a), and it does

TABLE 1. Qualitative staining intensity of plaque components

Plaque Component	Macrophages (KP-1)	ApoB-100 (MB47)	MDA-Lysine (MDA2)	OxPL (E06)	IK17	Apo(a) LPA4)
SMC-rich area[a]	−	+/−	+/−	+	+	+
Foamy macrophages	++/+++	−	+/−	++	++	+++
Lipid pools	+/−	+/++	+/++	++	++	+/++
Necrotic core	+++	+/−	+	++	+++	++
Fibrous cap macrophages	++	−	−	+++	++	+++

[a]Values represent evaluation in AIT, IX, and PIT only, as SMCs were present only in very limited numbers in more advanced atherosclerotic lesions.

not cross-react with plasminogen (23). All preparations were greater than 99% pure.

Immunohistochemistry

Formalin-fixed paraffin sections (5 μm) were incubated overnight at 4°C with primary antibodies MDA2, MB47, E06, and LPA4 at respective dilutions of 1:400, 1:50, 1:1,200, and 1:400. The detection of primary antibodies bound to their respective antigen was achieved using the biotinylated link antibody LSAB2 System-HRP DAB kit (Dako, Carpenteria, CA) with appropriate secondary antibodies directed to mouse IgG or IgM. Histologic sections for antibody staining against IK17 were initially incubated overnight with nonimmune goat anti-human IgG (GAH, Vector, BA-3000) at a dilution of 1:100 in 2% goat serum to reduce nonspecific background staining. For IK17 immunostaining, IK17 was diluted 1:600 in 2% goat serum and incubated for 1 h at room temperature (RT). Primary labeling was then visualized using an alkaline phosphatase-labeled goat anti-human secondary antibody (dilution 1:200, Sigma A3813) for 1 h at RT and visualized with Vector Red (Vector SK-5100).

For the identification of specific cell types, paraffin sections were immunostained for resident macrophages with anti-CD68 (KP-1) (dilution 1:400, M0814, Dako) and SMC with an anti-SMC α-actin (dilution 1:400, M0851, Dako). Both antibodies were visualized using an Envision+System-HRP (DAB) kit (Dako).

Assessment of immunolocalization of OSE, apo(a), and macrophage markers

The degree of MB47, MDA2, E06, LPA4, and IK17 and macrophage marker positivity was assessed qualitatively and quantitatively. Qualitative assessment within plaque components was performed on a scale of 0–3+: 0 (absent); + <10% of component area; ++ = 10–50% of component area; +++ > 51% of component area. Morphometric measurements of coronary sections were performed using image-processing software (IPLabs, Scanalytics, Rockville, MD) on slides stained with Movat Pentachrome. Quantitative planimetry with computer-assisted color image analysis segmentation with background correction quantified immunohistochemical stains of OSE for each antibody within regions of interest.

Total lipid extraction and LC-MS/MS of material from distal protection devices

All distal protection devices were of the filter variety (FilterWire EZ, 110 μm pores, Boston Scientific; Accunet Rx, 100 μm pores, Abbott). Filter material was subjected to a Folch lipid extraction with chloroform/methanol (2:1). For total lipid extraction, 500 μl of filter material homogenates was transferred into a glass tube, 2.5 ml of ice-cold chloroform/methanol and 17:1/17:1 PC were added as internal standards, and the tubes were vortexed at a maximum speed for 30 s. After centrifugation, the lower organic phase was transferred into a fresh glass tube using a Pasteur pipette, and the organic phase was dried under argon to ~200 μl and stored at −80°C.

Isocratic high performance liquid chromatography (HLPC) was carried out using a Shimadzu (Columbia, MD) LC-10AD high-performance pump interfaced with a Shimadzu SCL-10A controller. Sample was injected onto a 2.1 mm × 250 mm Vydac (Hysperia, CA) C18 column (Vydac catalog number 201TP52) held at 40°C using a Leap Technologies (Carrboro, NC) PAL autosampler. A buffer of isopropyl alcohol/water/tetrahydrofuran (40/40/20, v/v/v) with 0.2% formic acid at a flow rate of 300 μl/min was used for sample elution. The eluate was coupled to a mass spectrometer for further analysis. Separation optimization and verification of HPLC retention times were achieved using 16:0–05:0 (ALDO) PC standard.

All of the mass spectral analyses were performed using an Applied Biosystems (Foster City, CA) 4000 QTrap hybrid quadrupole linear ion trap mass spectrometer equipped with a Turbo V ion source, as previously described and validated (24). Protonated adducts of the 1-palmitoyl-2-(5′-oxo-valeroyl)-*sn*-glycero-3-phosphocholine (POVPC) were formed using the following settings: CUR, 10 psi; GS1, 40 psi; GS2, 0 psi; IS, 5500V; CAD, high; temperature, 500°C; ihe, ON; DP, 70V; CE, 35V; EP, 15V; and CXP, 15V. The 4000 QTrap is capable of carrying out tandem mass spectrometry, where a specified precursor ion (denoted by its mass-to-charge ratio, *m/z*) can be isolated in the first sector of the instrument, fragmented in a second sector collision cell, and the fragments produced then identified by their *m/z* in a third sector. A specialized form of tandem mass spectrometry is multiple reaction monitoring (MRM), in which multiple MRM

TABLE 2. Quantitative immunostaining of macrophages and oxidation markers by plaque composition and cell type

Cell Type and Plaque Component	KP-1	ApoB-100 (MB47)	MDA-lysine (MDA2)	OxPL (E06)	IK17	Apo(a) (LPA4)
SMC expression (% of α-actin)[a]	—	11.5	9.7	100	59	100
Foamy macrophage expression (% of KP-1 area)	—	25.2	10.4	100	100	100
Fibrous cap macrophages (% of KP-1 area)	—	100	56.6	100	100	100
Lipid pools (% of area)	1.1	6.3	1.0	4.7	5.6	24.8
Shoulder region (% of area)	8.2	1.4	1.0	13.8	9.7	17.5
Fibrous cap (% of area)	11.3	2.0	1.9	17.0	12.9	22.3
Necrotic core (% of area)	38.7	3.0	1.8	15.9	36.1	28.9

Values expressed as percentage of α-actin, KP-1, or plaque component.

[a]Values represent evaluation in AIT, IX, and PIT only, as SMCs were present only in very limited numbers in the progressive atherosclerotic lesions.

TABLE 3. Quantitative immunostaining of macrophages and oxidation markers by plaque type

Morphology	Macrophage (KP-1)	ApoB-100 (MB47)	MDA-lysine (MDA2)	OxPL (E06)	IK17	Apo(a) (LPA4)
Nonprogressive intimal lesions						
AIT (n = 7)	0.08 ± 0.02	0.05 ± 0.03	0.4 ± 0.2	0.8 ± 0.3	0.02 ± 0.02	1.5 ± 0.3
IX (n = 8)	19.4 ± 3.3	0.6 ± 0.4	0.8 ± 0.30	18.1 ± 5.1	5.4 ± 4.7	11.2 ± 5.9
Early progressive atherosclerotic lesions						
PIT (n = 11)	1.4 ± 0.6	3.0 ± 0.9	0.9 ± 0.7	3.6 ± 0.9	2.9 ± 1.5	14.3 ± 3.8
EFA (n = 25)	10.6 ± 1.5	1.8 ± 1.1	0.5 ± 0.1	5.3 ± 1.0	8.2 ± 1.6	11.8 ± 1.4
Late progressive atherosclerotic lesions						
LFA (n = 17)	11.8 ± 2.1	1.3 ± 0.3	1.0 ± 0.4	7.5 ± 1.9	12.9 ± 3.1	17.1 ± 3.4
TCFA (n = 13)	25.5 ± 3.6	3.6 ± 1.6	1.9 ± 0.6	18.0 ± 4.3	24.4 ± 4.8	31.1 ± 8.4
Plaque rupture (n = 8)	25.9 ± 6.5	2.0 ± 0.7	2.3 ± 0.7	25.6 ± 5.4	31.9 ± 4.9	30.1 ± 5.9
P value[a]	<0.0001	0.45	0.50	<0.0001	<0.0001	<0.0001

Values represent mean percentage (± SEM) positive stained area of macrophage and lipid oxidation marker within each coronary section classified by dominant lesion type.

[a]ANOVA, across all plaque types.

pairs can be monitored in a single analysis. In (+)ESI mode, the fragment produced by all protonated PC species, regardless of their parent mass or moiety, is the phosphocholine headgroup with *m/z* 184. Thus, in the same analysis, 16:0–05:0 (ALDO) PC were monitored employing the MRM pairs 650/184 and 664/184, respectively.

Statistical analysis

Mean variables between the various lesions were compared with one-way ANOVA (ANOVA; SPSS) followed by Student *t*-test for all differences among means. Spearman's correlation was used to demonstrate the relationship between macrophages and OSE. A value of $P \leqslant 0.05$ was considered statistically significant.

RESULTS

Qualitative and quantitative patterns of coronary artery immunostaining

Qualitative immunostaining patterns of macrophage, OSE, and apo(a) by plaque composition. The immunostaining patterns and intensity by plaque composition in all plaque types are displayed in **Table 1**. The macrophage marker KP-1 strongly stained foam cells and the necrotic core, as expected. ApoB-100, detected by MB47, was seen primarily in early lesions in lipid pools and in lesser amounts in SMC-rich areas and the necrotic core. Foamy macrophages did not stain for apoB-100 with MB47. Malondialdehyde (MDA) epitopes, detected by MDA2, demonstrated a similar pattern of staining as apoB-100 but showed some positivity in foamy macrophages. OxPL epitopes, detected by E06, were strongest in macrophage-rich areas, lipid pools, and the necrotic core. IK17 epitopes were strongest within necrotic cores and were mainly present in areas rich in foamy macrophages. Apo(a) epitopes, detected by LPA4, were consistently present throughout early and late lesions, especially in macrophages and the necrotic core.

Quantitative immunostaining patterns of macrophages and oxidation markers by plaque composition and cell type in all plaque types. Macrophage expression was primarily present in fibrous caps, shoulder areas, and the necrotic core (**Table 2**). ApoB-100 and MDA epitopes were primarily present in macrophage-rich areas in the fibrous cap and foamy macrophages, but they were almost absent in the necrotic core and shoulder regions. OxPL, IK17, and apo(a) epitopes were nearly uniformly expressed in SMC and macrophage-rich areas. IK17 epitopes were more prevalent in the necrotic core compared with the other epitopes. The fibrous cap expressed minimal apoB-100 and MDA epitopes, but OxPL, IK17, and apo(a) epitopes were present in 13–22% of the fibrous cap area.

Quantitative immunostaining patterns across plaque types and epitopes. Across plaque types. The extent of macrophage staining was most prevalent in TCFA and plaque rupture, less so in IX, EFA, and LFA, and minimally in AIT and PIT (**Table 3**). Macrophages were primarily present in the necrotic core and within the fibrous cap and increased with advancing plaque types. ApoB-100 and MDA staining was minimal in most lesion types, representing only 3–4% at most of total lesion area. Staining for apoB-100 was generally within the extracellular space, most prominent within areas of lipid pools and SMCs. OxPL and IK17 epitopes were strongly present in plaque rupture, TCFA, and IX, less so in PIT, EFA, and LFA, and virtually absent in AIT. The predominant site of OxPL staining was in the necrotic core and in foam cell macrophages. IK17 staining was most prominent in the necrotic core with strong positive staining also seen in macrophages. Apo(a) epitopes were strongly present in PR and TCFA, and they were modestly present in IX, PIT, EFA, and LFA, suggesting more nonspecific accumulation. Apo(a) staining was intense in the necrotic core, as well as in foam cell and nonfoamy macrophages. There was strong staining for OxPL, apo(a), and IK17 epitopes within the necrotic core of ruptured plaques (mean of total percentage OxPL, apo(a), and IK17 stained area, respectively, 60%, 57%, and 72%). OxPL and apo(a) were strongly expressed in foamy cell macrophages within the fibrous cap, whereas IK17 epitopes were mostly absent within viable macrophages.

Across epitope types. In normal coronary arteries with AIT, staining of macrophages and all OSE and apo(a) was negligible (data not shown). In contrast, IX contained few apoB-100 and MDA epitopes, significantly more macrophage, OxPL, and apo(a) epitopes, and fewer IK17

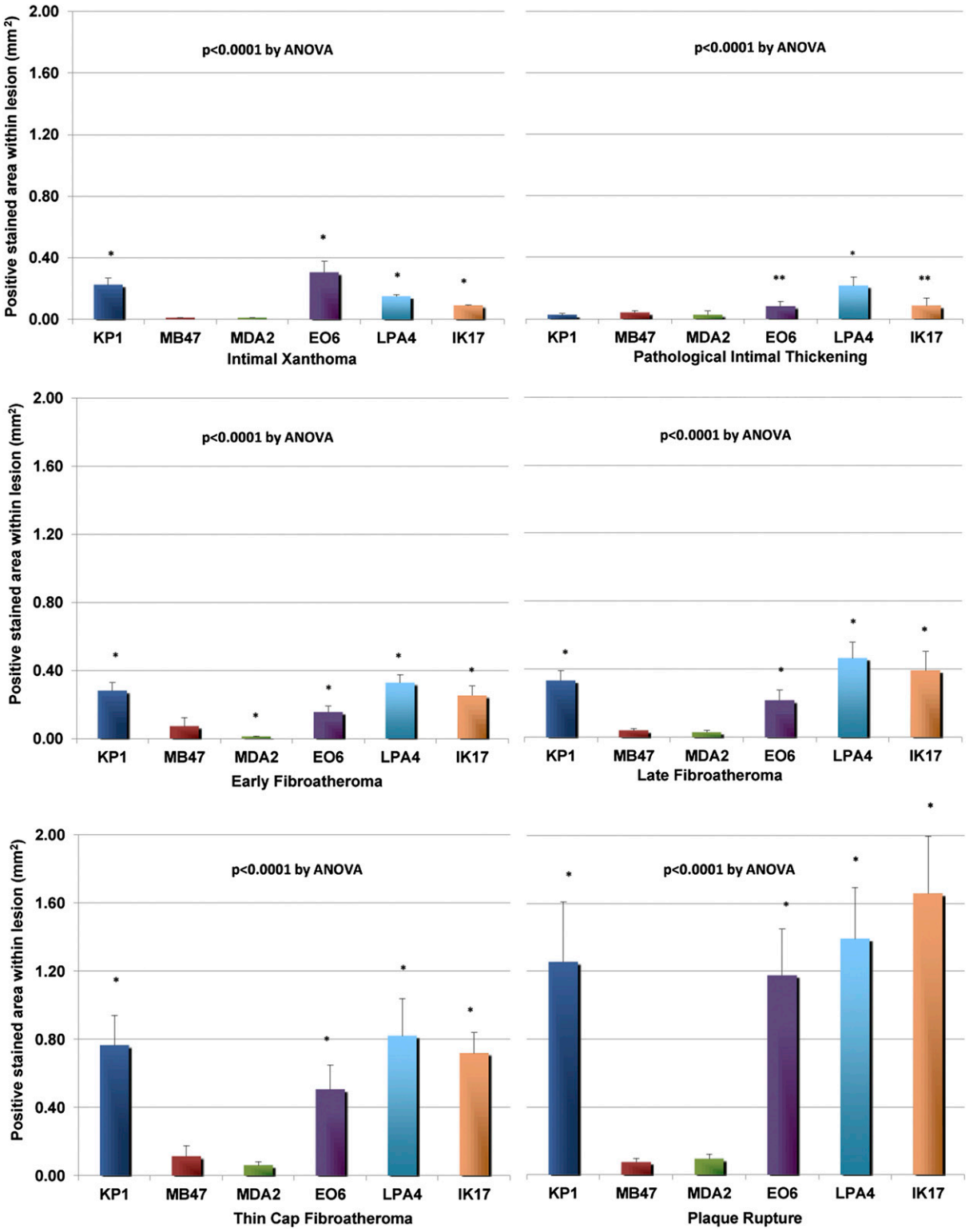

Fig. 1. Morphometric analysis of macrophages and OSE between IX and PIT, EFA, LFA, TCFA, and ruptured plaques. Bars represent mean values (± SEM) of positively stained area (mm^2) of macrophages (KP-1) and lipid/oxidation markers. *$P < 0.001$, **$P < 05$ compared with MB47 by posthoc Bonferonni correction of one-way ANOVA.

epitopes (**Fig. 1**). PIT lesions were enriched in apo(a) epitopes. EFA and LFA were strongly positive for macrophages, OxPL, IK17, and apo(a) epitopes, whereas TCFA and plaque ruptures showed enhanced staining for macrophages, OxPL, apo(a), and IK17 epitopes. Significant differences were noted in expression of epitopes in all six lesion types by ANOVA (all $P < 0.0001$). In posttest Bonferonni analysis among paired comparison of epitope types, in general, significant differences were not present between apoB and MDA2 epitopes, but they were present

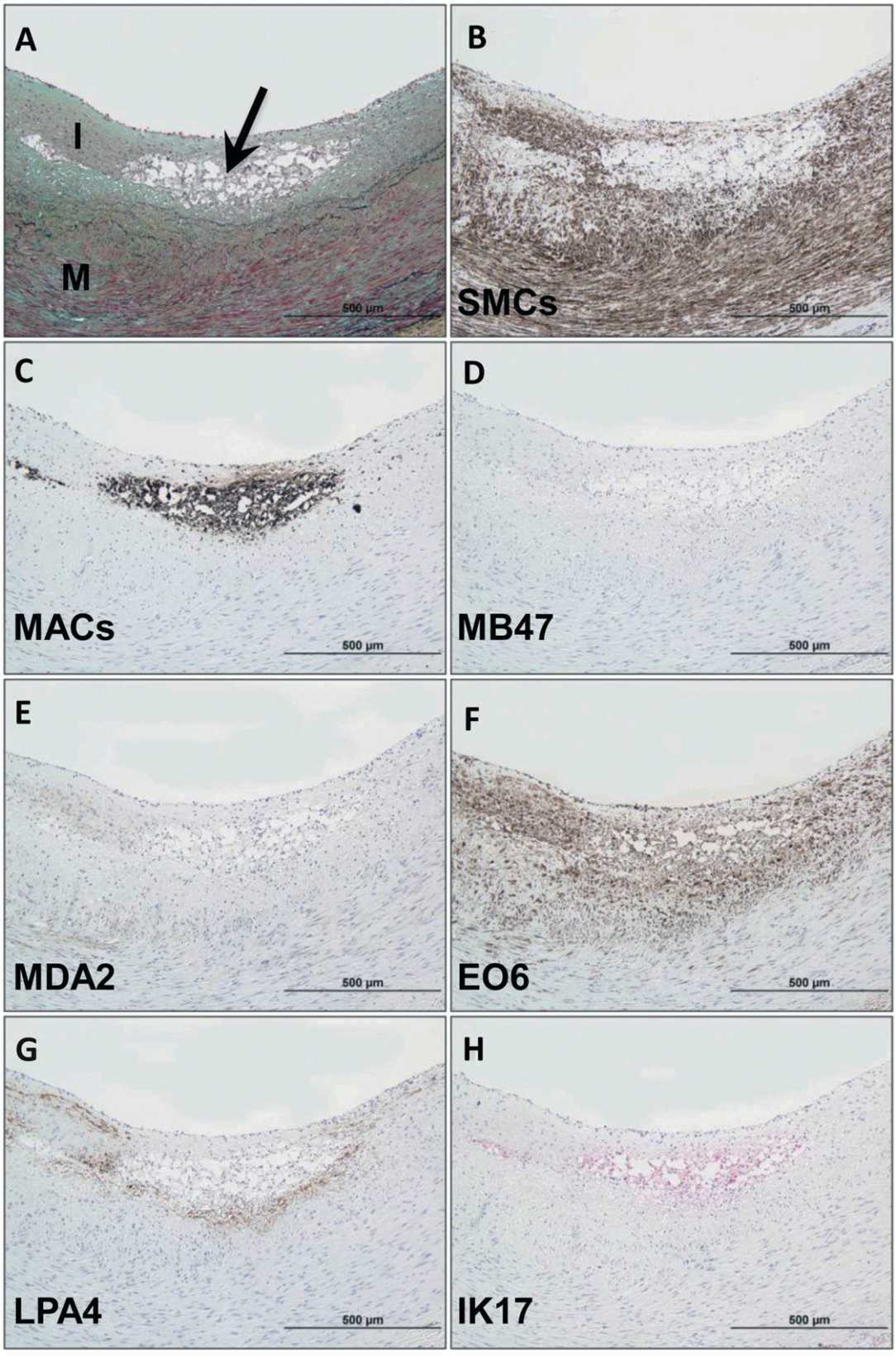

Fig. 2. Immunostaining of OSE in a human coronary intimal xanthoma. A: Intimal xanthoma recognized as an early superficial lesion rich in macrophages without evidence of necrosis. Arrow, Movat pentachrome; I, intima; M, media) B: Areas of SMC (anti-SMC α-actin). C: Localization of CD68 staining for macrophages, which do not overlay regions of SMCs. D, E: Relative absence of staining for apoB-100 (MB47) and MDA epitopes (MDA2), respectively. F: Strongly positive OxPL (E06) staining colocalizes with macrophages and nearby SMCs of the neointima. G, H: apo(a) (LPA4) and IK17 epitopes, respectively, are expressed in select populations of macrophages. B–G: Immunoperoxidase (brown reaction product). H: Alkaline phosphatase (red reaction product). Magnification ×200.

among OxPL, apo(a), and IK17 epitopes (ranging from $P < 0.05$ to $P < 0.001$).

Morphometric patterns of immunostaining

Intimal xanthoma. Immunostaining of normal segments of coronary arteries revealed no staining with any of the oxidation-specific monoclonal antibodies, but there was occasional minimal endothelial cell staining noted with monoclonal antibody LPA4 for apo(a) epitopes. Immunostaining of an intimal xanthoma (**Fig. 2**) shows an early superficial lesion rich in macrophages without evidence of necrosis. There is a relative absence of staining for apoB-100 and MDA epitopes but strong positive staining for OxPL, which are present in areas rich in macrophages and SMCs. IK17 and apo(a) epitopes are expressed in select populations of macrophages in a distribution different from E06.

Pathologic intimal thickening. Immunostaining of pathologic intimal thickening (**Fig. 3**) shows a superficial plaque with an acellular lipid pool in a proteoglycan-rich matrix. SMCs are mostly present in the medial wall and superficial layers outside the lipid pool, whereas macrophages are present above the regions of the lipid pool. There is moderate staining for apoB-100 but intense staining for apo(a) in areas of the lipid pool. Staining for MDA epitopes is essentially negative. OxPL staining is primarily present in areas of superficial macrophages and SMCs above the area of the lipid pool, whereas weak to moderate staining for IK17 epitopes is seen in the lipid pool.

Early fibroatheroma. Immunostaining of an early fibroatheroma (**Fig. 4**) shows a superficial plaque with an early necrotic core characterized by macrophages, free cholesterol, and extracellular matrix. SMCs are mostly present in the medial wall and fibrous cap, whereas macrophages stain intensely in the fibrous cap and necrotic core. Staining for apoB-100 and MDA epitopes is essentially negative. OxPL are primarily present in areas rich in macrophages in the fibrous cap, whereas weak to moderate staining for IK17 epitopes is seen in the necrotic core. Expression of apo(a) is primarily localized to the extracellular matrix of the fibrous cap.

Late fibroatheroma. Immunostaining of a late fibroatheroma (**Fig. 5**) shows an intact thick fibrous cap overlying a late necrotic core characterized by cell debris, free cholesterol, and relative absence of extracellular matrix. SMCs are present in the media and superficial area of the fibrous cap. Macrophages are mainly present in the necrotic core and pericore regions, with some infiltration in the fibrous cap. There is relatively weak staining for apoB-100 in the region of the necrotic core, and MDA epitopes are essentially absent. OxPL and apo(a) epitopes show a similar distribution and are found primarily in the extracellular matrix of the fibrous cap and necrotic core. IK17 epitopes are strongly positive in the necrotic core and absent elsewhere.

Thin cap fibroatheroma. Immunostaining of a thin cap fibroatheroma (**Fig. 6**) shows an intact thin fibrous cap overlying a late necrotic core. SMCs are conspicuously absent in the fibrous cap but present in the media and intimal/medial interface. There is marked infiltration of macrophages in the thin fibrous cap and underlying necrotic core. ApoB-100 is predominantly localized to the necrotic core and surrounding acellular areas, and MDA epitopes are seen in similar areas, except the intensity of staining is markedly weaker. OxPL are primarily present in the fibrous cap rich in macrophages and in the extracellular matrix, including in the periphery of the necrotic core. There is intense staining for apo(a) in the fibrous cap and regions of the necrotic core, mostly in the extracellular matrix. IK17 is strongly positive in the late necrotic core.

Plaque rupture. Immunostaining of plaque rupture (**Fig. 7**) shows a coronary lesion with fibrous cap disruption and superimposed luminal thrombus. SMCs are present in the medial layer but not in the plaque. In contrast, there is marked infiltration of macrophages in the fibrous cap and underlying necrotic core. Staining for apoB-100 is essentially negative. MDA epitopes are moderately expressed in the fibrous cap within cells and extracellular matrix and necrotic core. OxPL are primarily localized to macrophages in the periphery of the necrotic core. There is intense reaction to apo(a) in the disrupted fibrous cap overlying the necrotic core. IK17 epitopes are present only in the late necrotic core.

Presence of OSE in carotid endarterectomy specimens

We also studied carotid endarterectomy specimens that were surgically removed en bloc and then immediately fixed in neutral buffered formalin. Remarkably, these carotid lesions displayed findings very similar to those observed with the coronary lesions. An example of immunostaining of a carotid TCFA with a necrotic core and presence of macrophages signifying the presence of OSE is shown in **Fig. 8**. Similar to the findings in the coronary arteries, apoB and MDA epitopes were predominantly localized to the less lytic areas of necrotic core. However, OxPL, apo(a) and IK17 epitope staining was strongly positive within macrophages and the necrotic core.

Presence of OxPL in carotid and coronary SVG distal protection devices documented by LC-MS/MS

To obtain physical evidence for the presence of oxidized lipids in these necrotic lesions, we collected plaque material released from such lesions during interventional procedures and trapped by distal protection devices. The filters were placed in potent antioxidants, frozen at −70°C, and then lipid extracted and examined by LC-MS/MS for the presence of OxPL. Protonated adducts of 1-palmitoyl-2-(5′-oxo-valeroyl)-*sn*-glycero-3-phosphocholine (POVPC) (*m/z* 594), a well validated bioactive, pro-inflammatory and pro-atherogenic OxPL (25, 26) that reacts with E06 (27), were detected from both carotid and coronary distal SVG protection devices (**Fig. 9**). This finding demonstrated

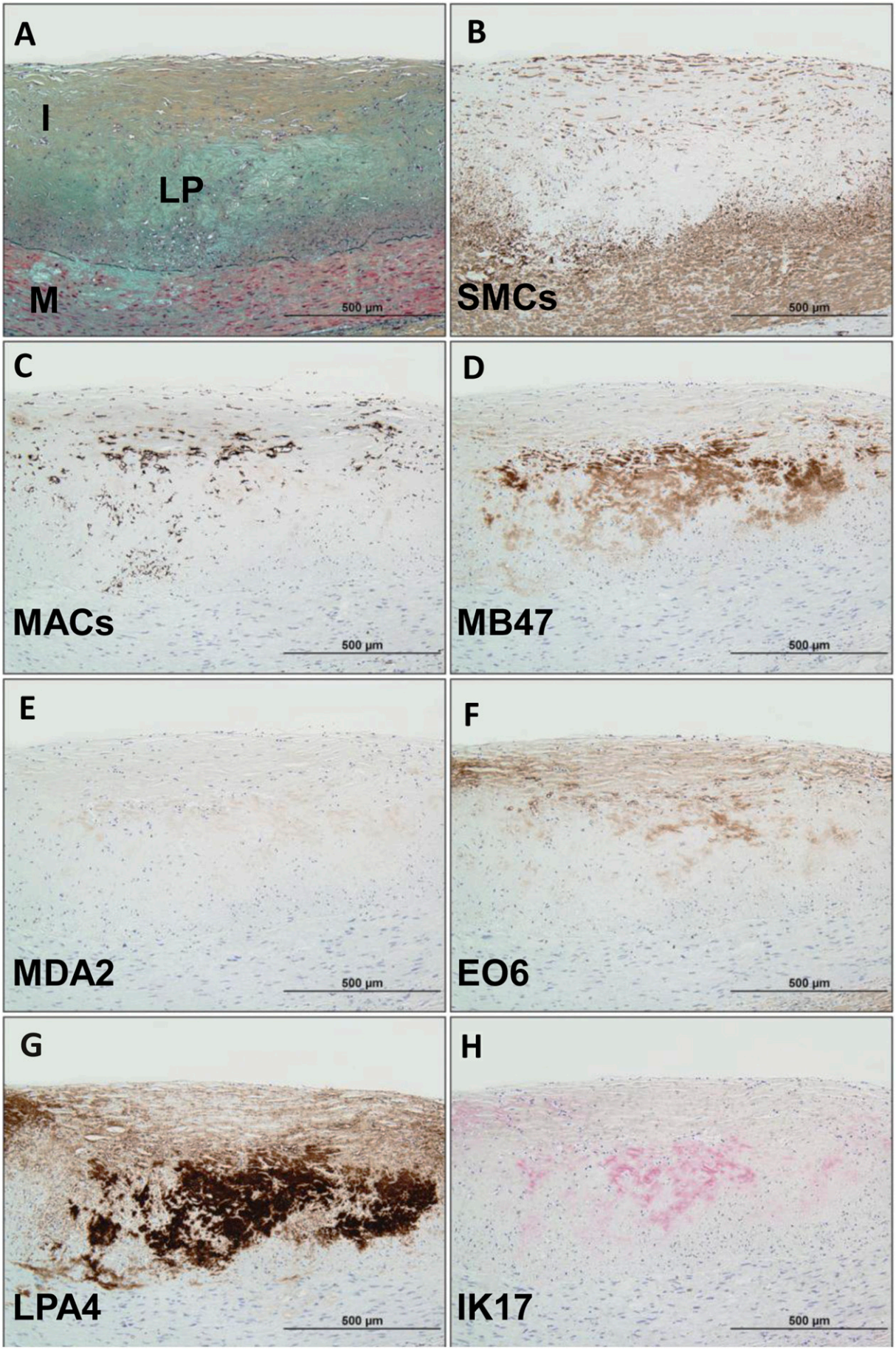
A
I
LP
M
500 μm
B
SMCs
500 μm
C
MACs
500 μm
D
MB47
500 μm
E
MDA2
500 μm
F
EO6
500 μm
G
LPA4
500 μm
H
IK17
500 μm

that the OxPL detected in both the coronary and carotid lesions by E06 immunostaining represented epitopes present in vivo and not products of artifactual oxidation that occurred during tissue processing.

Effect of time to harvest and expression of OSE

Immunostaining of freshly procured carotid endarterectomy specimens stored at room temperature for 24 h, on ice for 24 h, or in antioxidants for 24 h demonstrated no appreciable qualitative differences in immunostaining patterns among antibodies with different methods of storage prior to analysis (**Fig. 10**).

DISCUSSION

This is the first comprehensive analysis evaluating several well-characterized OSE and apo(a) in a wide range of human coronary, carotid, and SVG atherosclerotic lesions. The study demonstrates a differential expression of apoB-100, OSE, and apo(a) in the progression of atherosclerosis from early lesions to plaque rupture. Plaques that develop during early atherosclerosis are enriched in apoB-100, apo(a), and all the OSE measured in this study. However, as lesions progress, apo(a), OxPL, and IK17 epitopes become progressively enriched. Specifically, apo(a) epitopes were present in most lesions, whereas OxPL and IK17 epitopes were mainly associated with foamy macrophages of the fibrous cap and the necrotic core. IK17 epitopes were most specifically associated with necrotic cores and plaque rupture. Additionally, a similar distribution was noted in TCFA of freshly procured carotid endarterectomy specimens. Finally, LC-MS/MS documented the presence of OxPL in material trapped by distal protection devices, documenting their presence in vivo in clinically symptomatic plaques. These observations provide a framework for understanding the relationship between OSE and Lp(a) and the progression and destabilization of human coronary and carotid atherosclerosis.

This study used unique monoclonal antibodies targeting well-characterized lipoprotein and OSE to study their relationship to human atherosclerosis, as described in Methods. For example, MB47 detects not only the native apoB-100 moiety of unoxidized LDL but also apoB of minimally oxidized LDL and even apoB fragments of extensively oxidized LDL. MDA2 can recognize both MDA-LDL as well as MDA-lysine epitopes on other proteins in the vessel wall, such as apoAI (28, 29), and it has also been utilized for noninvasive imaging of experimental atherosclerotic lesions (3–5). E06 is a well-characterized murine IgM natural antibody cloned from apoE$^{-/-}$ mice (20) that has previously been used to stain mouse and rabbit atherosclerotic lesions and to image atherosclerotic lesions in apoE$^{-/-}$ mice using magnetic resonance techniques (3–5). E06 is also used in plasma immunoassays to detect OxPL on circulating apoB-100 particles (OxPL/apoB) in humans (10). In support of these pathologic findings, plasma levels of the OxPL epitopes on apoB-100 particles (OxPL/apoB) measured by E06 were recently shown to be strongly associated with the presence of angiographically defined coronary artery disease, to predict the presence and progression of carotid and femoral atherosclerosis, and to predict cardiovascular death, myocardial infarction, and stroke in unselected epidemiological populations (30, 31). LPA4 binds to the apolipoprotein(a) portion of Lp(a) and is used in immunoassays to measure plasma Lp(a) levels, but it has not been previously used to immunostain tissues (23). Apo(a) itself is not an oxidation-specific epitope, but apo(a) and Lp(a) bind OxPL, which may reflect the key atherogenic component of Lp(a) (32). IK17 is a human Fab fragment derived from a phage display library, and it binds to a unique MDA-like epitope present on both MDA-LDL and copper-oxidized LDL. IK17 has also been used in detecting and imaging atherosclerosis in LDLR$^{-/-}$ mice and apoE$^{-/-}$ mice (3–5, 22).

The differences in immunoreactivity patterns present among the different antibodies suggest that specific epitopes are generated and/or enriched during different pathophysiological stages of lesion development, progression, and destabilization. Such epitopes can be generated through peroxidation of unsaturated fatty acids present on lipoproteins, phospholipids, and cell membranes in the vessel wall, as well when cells, such as macrophages, undergo apoptosis. Despite the fact that these epitopes are generated through oxidative modification, expression of specific epitopes appears dependent on the stage of lesion progression. For example, MDA epitopes were more common in early lesions, such as in PIT and early fibroatheromas, whereas OxPL, apo(a), and IK17 epitopes were more prevalent in advanced lesions. Most of the prior data with antibody MDA2 were generated in mouse and rabbit models, with early to intermediate lesions showing diffuse staining patterns both intra- and extracellularly (33). MDA2 has been used to stain early lesions in teenage subjects in the Bogalusa Heart Study (34). Surprisingly, in the current study, MDA epitopes did not become more prevalent as lesions advanced. It may be postulated that MDA epitopes are generated early in the development of atherosclerosis and may more closely reflect plaque initiation and plaque accumulation rather than plaque destabilization. It is also possible that there is decomposition of these epitopes in more aged tissues. We have recently shown that complement factor H also binds MDA epitopes, both

Fig. 3. Immunostaining of OSE in a human coronary lesion recognized as pathologic intimal thickening. A: Human coronary lesion shows a superficial plaque with an acellular lipid pool (LP) rich in proteoglycan matrix. Movat pentachrome; I, intima; M, media. B: α-Actin-positive SMCs are mostly localized to the medial wall and superficial layers outside the LP. C: Localization of CD68 staining shows few positive macrophages above the regions of the LP. D: Moderate staining for MD47 is noted for superficial macrophages and deeper areas of the LP. E: MDA2 expression is essentially negative. F: E06 is found primarily localized to superficial macrophages and SMCs above the area of the LP. G: Intense reaction against LPA4 primarily localized to the region of the LP. H: Weak to moderate staining of IK17 is seen in the LP. B–G: Immunoperoxidase (brown reaction product). H: Alkaline phosphatase (red reaction product). Magnification ×200.

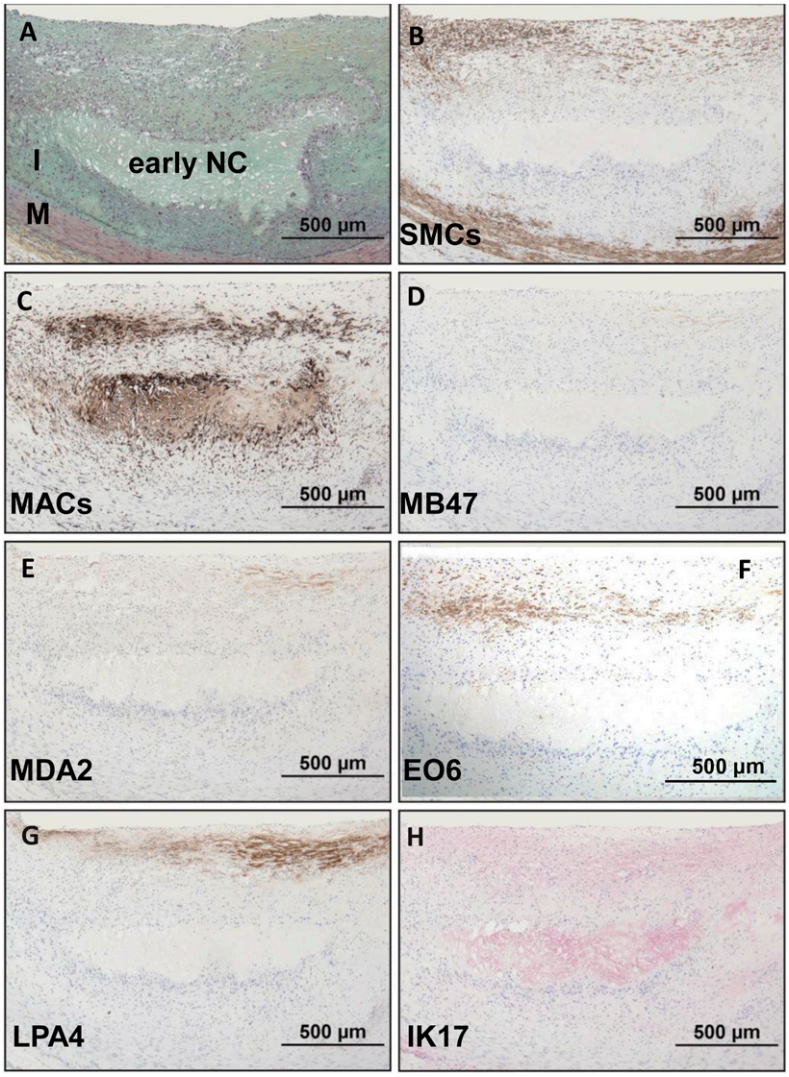

Fig. 4. Immunostaining of OSE in a human coronary lesion recognized as early fibroatheroma. A: Human coronary lesion shows a superficial plaque with an early necrotic core (NC) characterized by macrophages, free cholesterol, and extracellular matrix. Movat pentachrome; I, intima; M, media. B: α-Actin-positive SMCs are mostly localized to the medial wall and fibrous cap. C: Localization of CD68 staining shows positive intense macrophage staining of the fibrous cap and necrotic core. D, E: Negative staining for MD47 and MDA2, respectively. F: E06 is found primarily localized to macrophages of the fibrous cap. G: Expression of LPA4 is primarily localized to the extracellular matrix of the fibrous cap. H: Weak to moderate staining of IK17 is seen in the necrotic core. B–G: Immunoperoxidase (brown reaction product). H: Alkaline phosphatase (red reaction product). Magnification ×200.

in the eyes of patients with macular degeneration and in human coronary atherectomy specimens (35). In fact, prior side-by-side staining of such tissues with anti-CFH antibodies and MDA2 has shown partial colocalization but also independent staining. It is possible that CFH may bind and mask some of these epitopes. It is also possible that these epitopes may be bound by autoantibodies to MDA-LDL that have been well characterized (36). Additionally, some of these epitopes may be transported out of the lesion wall on migrating macrophages or lipoproteins.

In contrast, apo(a), OxPL, and IK17 epitopes were highly prevalent in foamy macrophages in thin fibrous caps, necrotic cores, and ruptured plaques, suggesting that they more closely reflect advancing and unstable plaques. In conjunction with these findings in late lesions, there was also a similarly increased expression of macrophage markers and a lack of SMC, consistent with the pathophysiological findings of plaque vulnerability. Thus, the expression of apo(a), OxPL, and IK17 epitopes may more closely reflect plaque inflammation, destabilization, and rupture. Some variability was noted in the earlier stage coronary lesions in cell-associated OxPL staining, and some of this may be due to destruction of OxPL epitopes as lesions progress. Alternatively, changes in extracellular matrix components in later stage lesions may allow greater accumulation of noncell-associated epitopes. Similarly, although both the carotid and coronary plaque are considered TCFA, the extent of macrophages, particularly in the cap region, appears much greater for the carotid, and E06 staining is present both in the macrophages of the cap and cap ECM, whereas relatively less in the necrotic core. These data in human lesions that span a broad array from early lesions to plaque rupture can only be tangentially compared with animal data in which most lesions studied are at the fatty-streak level. Nonetheless, the staining patterns for equivalent lesions seem similar, and these epitopes are equally expressed in animals and humans and are not species specific, but specific to the oxidative pathways generating these epitopes.

The origin and generation of the OSE merits some discussion. ApoB-100 is present on VLDL, VLDL remnants (IDL), LDL, and Lp(a). Once such apoB-containing lipoproteins enter the arterial intima, they bind to extracellular matrix (37) and then undergo oxidation mediated by a variety of free radical-mediated mechanisms. This likely

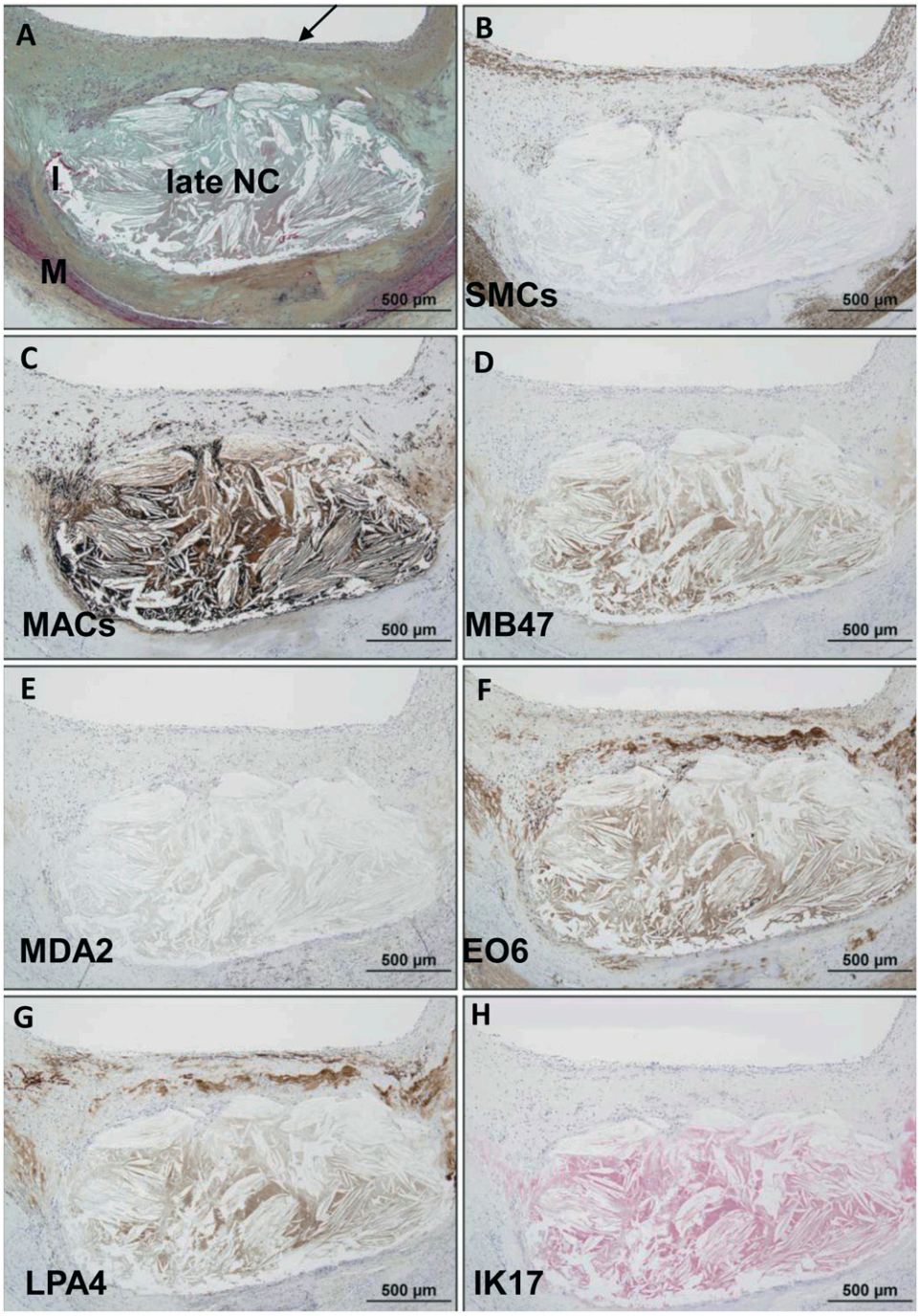

Fig. 5. Immunostaining of OSE in human coronary fibroatheroma with late necrosis. A: Human coronary lesion with an intact thick fibrous cap (arrow) overlying a late necrotic core (NC) characterized by cell debris, free cholesterol, and relative absence of extracellular matrix. Movat pentachrome; I, intima; M, media. B: α-Actin staining for SMCs is positive in the media and superficial area of the fibrous cap. C: Localization of CD68 staining shows infiltration of macrophages within the fibrous cap but mostly necrotic core and pericore regions. D: Relatively weak staining for MD47 in the region of the necrotic core. E: MDA2 expression is negative. F: E06 is found primarily localized to the extracellular matrix of the fibrous cap and necrotic core. G: Staining intensity and localization of LPA4 is similar to E06 in (F). H: IK17 is strongly positive in the NC. B–G: Immunoperoxidase (brown reaction product). H: Alkaline phosphatase (red reaction product). Magnification ×200.

explains the presence of apoB and MDA epitopes in relatively early lesions. As plaques progress, macrophage number and activation increase, which among other properties, leads to further oxidation of LDL, resulting in progressive lipid oxidation and accumulation of OxPL and IK17 epitopes. IK17 epitopes, which appear primarily in the necrotic core where macrophage foam cells and necrotic debris have accumulated, may represent a byproduct of very advanced oxidation of MDA-related adducts. Interestingly, prior attempts in our laboratory to detect

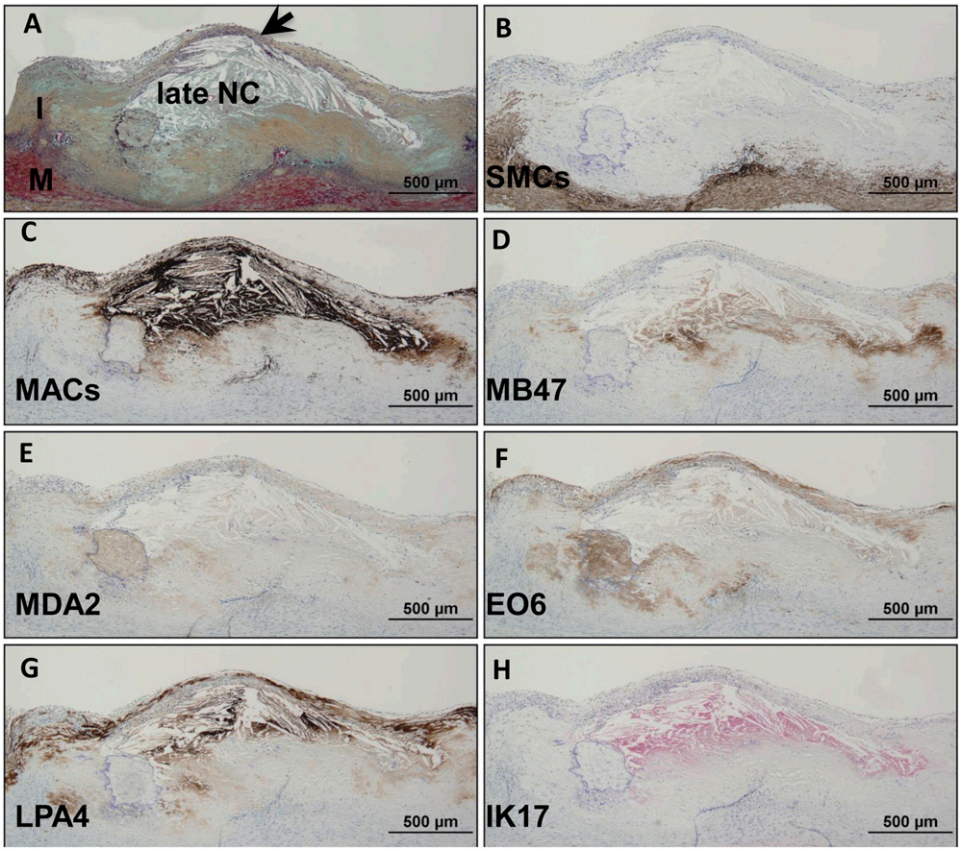

Fig. 6. Immunostaining of OSE in human coronary TCFA or high-risk plaque for rupture. A: Human coronary lesion with an thin intact fibrous cap (arrow) overlying a late necrotic core (NC). Movat pentachrome; I, intima; M, media. B: α-Actin staining for SMCs is positive in the media and intimal/medial interface, whereas the majority of plaque, in particular the fibrous cap, is negative. C: Localization of CD68 staining shows marked infiltration of macrophages in the thin fibrous cap and underlying necrotic core. D: Staining for MD47 is predominantly localized to the necrotic core and surrounding acellular areas. E: MDA2 expression is seen in similar areas as in (D), except the intensity of staining is markedly weaker. F: E06 is found primarily localized to fibrous cap macrophages and extracellular matrix including in the periphery of the necrotic core. G: Intense reaction against LPA4 is seen in the fibrous cap and regions of the necrotic core, mostly in the extracellular matrix. H: IK17 is strongly positive in the late NC. B–G: Immunoperoxidase (brown reaction product). H: Alkaline phosphatase (red reaction product). Magnification ×200.

IK17 epitopes on circulating lipoproteins, which appear to reflect advanced MDA-related epitopes, have been unsuccessful (S. Tsimikas, unpublished observations), suggesting that they may only be present in highly oxidized lipids and modified proteins within advanced lesions. It is important to note that both E06 and IK17 bind to apoptotic cells and apoptotic debris (2, 22), which are clearly enriched in late lesions and a major contributor to the unstable plaque. Indeed, Lp(a) and the OxPL it contains are likely to be a major stimulus leading to macrophage apoptosis and cell death (24). Further studies are needed to define the pathways through which these various OSE are generated in vivo.

In the current study, it was clearly demonstrated that Lp(a) is quite ubiquitous in atherosclerotic plaques, even in early lesions, and that it progressively increases as lesions progress to plaque rupture. The fact that apoB, apo(a), and OxPL did not necessarily uniformly colocalize suggests that the apoB and OxPL components of Lp(a) may be degraded and removed but that the apo(a) component continues to be bound to the plaque and have a longer residence time (38). It also suggests that additional and quantitatively significant amounts of OxPL are formed in the vessel wall in situ and independently of those OxPL potentially carried by Lp(a). Consistent with the current findings of the enhanced presence of Lp(a) in vulnerable plaques, a correlation was previously noted with plasma Lp(a) levels, apo(a) immunopositivity in atherectomy specimens, and the severity of the clinical presentation in patients with acute coronary syndromes (39). Indeed, as noted above, Lp(a) may well promote macrophage cell death via a CD36/TLR2-dependent process, thus contributing to plaque rupture (24). With the confluence of data showing that Lp(a) is an independent and potentially causal risk factor for cardiovascular disease (40, 41) and with emerging therapeutic interventions to lower Lp(a) (42–44 and B. C. Kolski and S. Tsimikas, unpublished observations), these data provide a scientific rationale why Lp(a) may contribute to both plaque progression and plaque destabilization, and they validate potential therapeutic targeting approaches.

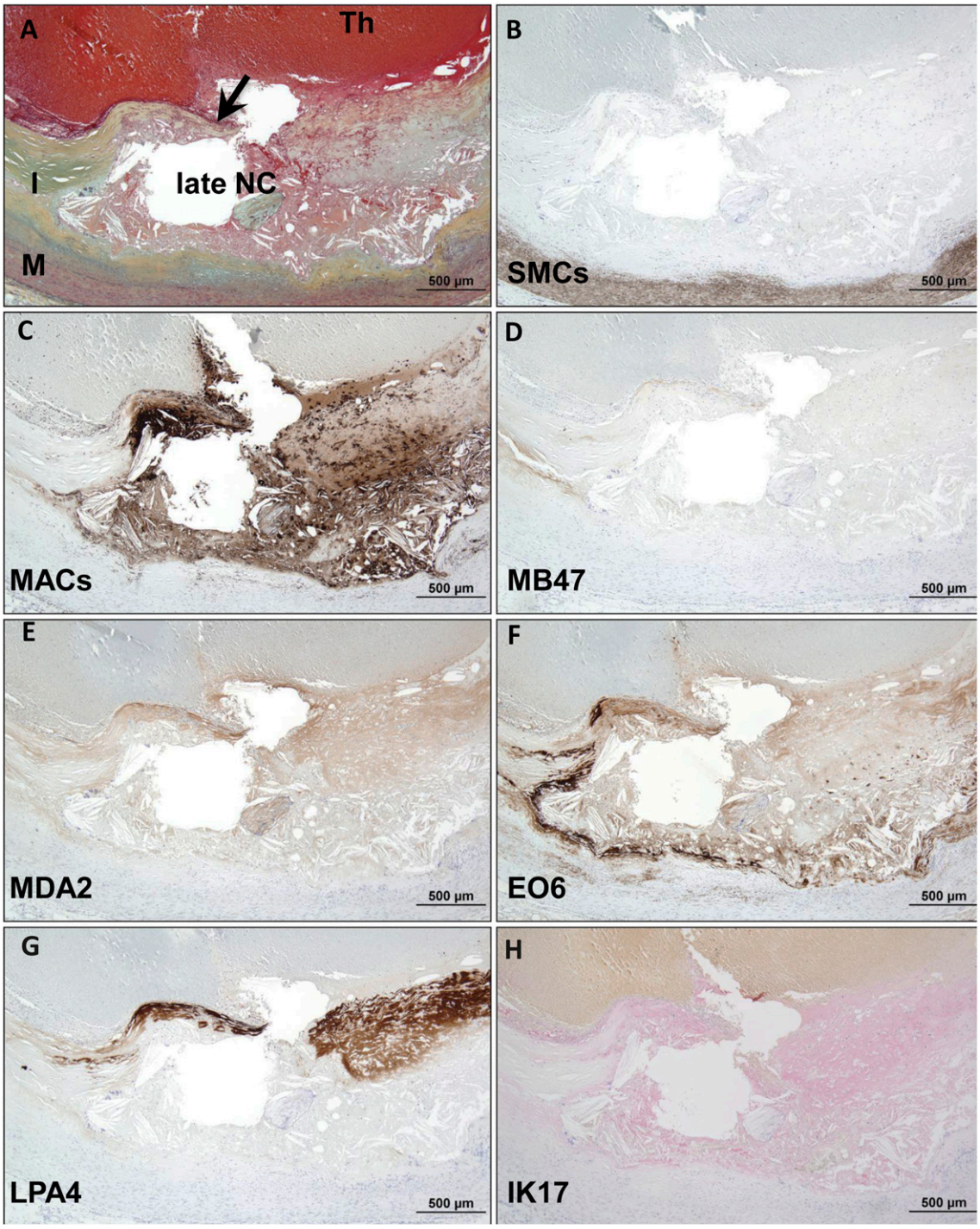

Fig. 7. Immunostaining of OSE in human coronary plaque rupture. A: Human coronary lesion with fibrous cap disruption (arrow) and superimposed luminal thrombus (Th, arrow). Movat pentachrome; I, intima; M, media. B: α-Actin staining for SMCs is positive in the medial layer but negative in the plaque. C: Localization of CD68 staining shows marked infiltration of macrophages in the fibrous cap and underlying late necrotic core (NC). D: Staining for MD47 is essentially negative. E: MDA2 expression is moderately expressed in the fibrous cap within cells and extracellular matrix and necrotic core. F: E06 is found primarily localized to macrophages in the periphery of the necrotic core. G: Intense reaction against LPA4 is seen in the disrupted fibrous cap overlying the necrotic core. H: Weak to moderate staining of IK17 is seen in the late NC. B–G: Immunoperoxidase (brown reaction product). H: Alkaline phosphatase (red reaction product). Magnification ×200.

Limitations

Artifactual oxidation may have occurred during procurement of the coronary specimens due to delay in harvesting after sudden death, and it may have impacted the findings in the later stage lesions. However, this cannot explain the findings with the carotid or SVG, as they were processed immediately in EDTA/BHT and handled optimally subsequently to maximally limit artifactual oxidation.

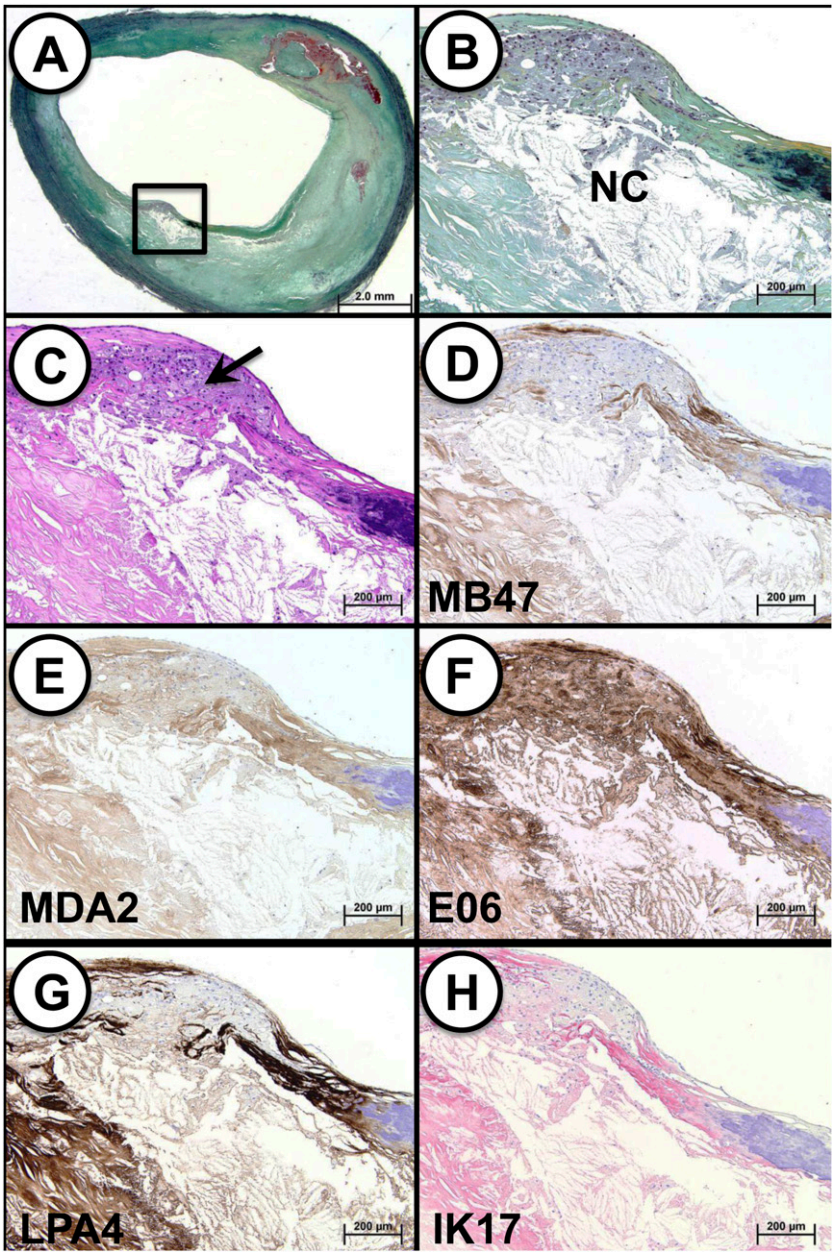

Fig. 8. Immunostaining of OSE in human carotid TCFA. A: Low-power view of a TCFA (Movat pentachrome); note the insignificant clinical stenosis. B: Higher power view of the region represented by the black box in (A) showing a necrotic core (NC) with a overlying intact thin fibrous cap, which is partially degraded by infiltrating macrophages. C: Cluster of macrophages within the fibrous cap (arrow; H and E staining). D: Immunostaining for MD47 is predominantly localized to the less lytic areas of necrotic core (lower left) and extracellular matrix of the fibrous cap; there is a relative absence of staining within fibrous cap macrophages. E: MDA2 expression is diffusely present in the fibrous cap, including macrophages and less lytic areas of the necrotic core; the staining intensity is the weakest of the five OSE epitopes. F: EO6 is strongly positive within the fibrous cap, including macrophages, as well as connective tissue and necrotic core. G: Immunostaining against LPA4 is intense in the less lytic areas of the necrotic core and connective tissue matrix. H: Staining pattern for IK17 mirrors that of LPA4 in which a strong signal is noted in the less lytic areas of the necrotic core and connective tissue matrix. D–G: Immunoperoxidase (brown reaction product). H: Alkaline phosphatase (red reaction product). A: Magnification ×10.25. B–H: Magnification ×100.

In these specimens, we saw the same pattern of OSE expression. In addition, the fact that MDA epitopes did not increase with lesion size and that the experimental study of various exposures of carotid endarterectomy specimens showed no major differences in immunostaining suggests that if postmortem oxidation did occur in the coronary specimens, it did not significantly impact the findings.

Clinical implications and conclusions

This comprehensive analysis of a range of human plaque types and stages of atherosclerosis demonstrates that OSE,

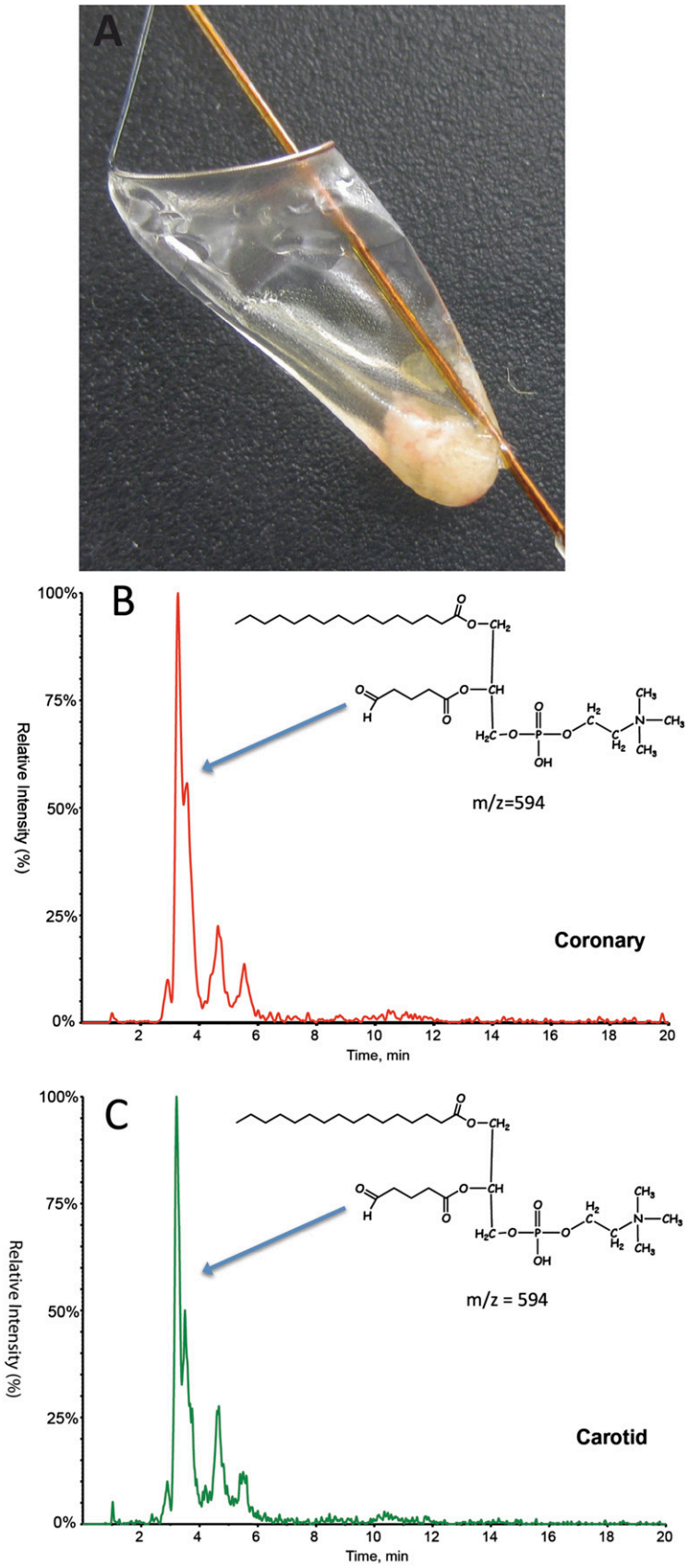

Fig. 9. A: Atheroemboli captured in a FilterWire following SVG intervention. B, C: LC-MS/MS multiple reaction monitoring (MRM) analysis of 1-palmitoyl-2-(5′-oxo-valeroyl)-*sn*-glycero-3-phosphocholine (POVPC) ($m/z = 594$) identified in atherosclerotic debris recovered from distal embolic protection filters following percutaneous angioplasty and stent placement of coronary SVG (B) and internal carotid artery (C). The later eluting, lower intensity peaks are due to stereoisomer effects.

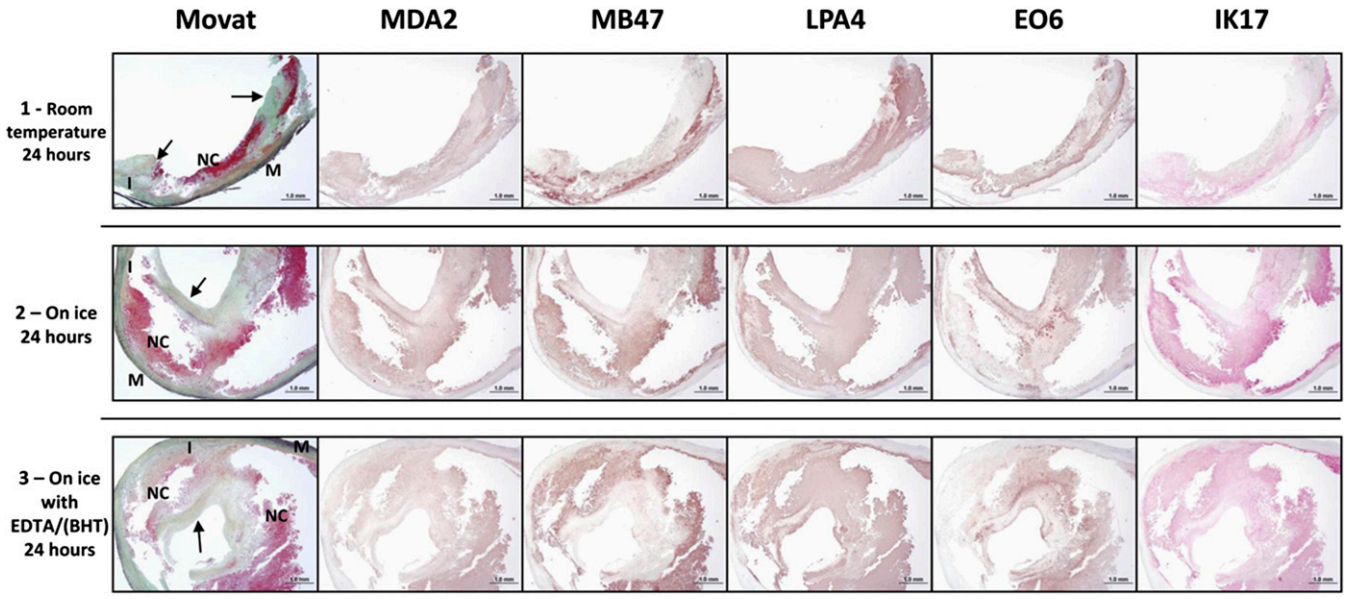

Fig. 10. Immunostaining of oxidation-specific epitopes represented by antibodies MDA2, MB47, LPA4, EO6, and IK17 of fresh human carotid endarterectomy specimens. Prior to paraffin embedding, the endarterectomy specimens were manually cut into three sections (proximal, mid, distal) because the specimens were not symmetrical, and due to some fragmentation during removal, the immunostained sections are of different size. Specimens were then handled according to the following procedures: (Row 1) Proximal specimen stored at room temperature for 24 h in PBS (phosphate buffered saline. Staining for MDA2 is weakly present in predominantly the necrotic core. MB47 staining is more intense and seen in similar areas as for MDA2. Expression of LPA4 and EO6 is located in the extracellular matrix regions of the fibrous cap and the necrotic core. IK17 is positive in the late necrotic core. Fibrous cap (arrows) adjacent and partially overlying a late necrotic core (NC). Movat pentachrome; I, intima; M, media. (Row 2) Mid specimen stored on ice for 24 h in PBS. MDA2 expression is present within the necrotic core. MB47 expression is more intense and is located within the areas as seen in the MDA2 staining. The localization of LPA4 and EO6 expression is similar as described for row 1, mostly in the extracellular matrix regions of the fibrous cap and the necrotic core. IK17 is strongly positive in the large late necrotic core. (Row 3) Distal specimen stored on ice in EDTA/BHT antioxidant for 24 h. MDA2 is weakly present in the necrotic core, whereas MB47 expression is more intense. Expression of LPA4 and EO6 is mostly seen in the extracellular matrix regions of the fibrous cap and the necrotic core, and the intensity of the staining is comparable to the staining in row 2. IK17 is strongly present in the late necrotic core. MDA2, MB47, LPA4, EO6: Immunoperoxidase (brown reaction product). IK17: Alkaline phosphatase (red reaction product). Magnification ×100.

in particular those detected by antibodies E06, IK17, and LPA4, are highly prevalent and progressively enriched in advancing atherosclerotic lesions and ruptured plaques. Several translational "biotheranostic" (biomarker, therapeutic, and diagnostic imaging) approaches targeting OSE, such as in-vitro assays, in-vivo and noninvasive diagnostic imaging modalities, and therapeutic applications have reached the investigational clinical frontier (9, 11, 12). As these studies ultimately make their way to clinical applications, the data generated in this study will provide a foundation for appropriate clinical applications and interpretation of the findings. Furthermore, the presence of vasoactive OxPL within distal protection devices is consistent with our prior data showing increased OxPL in plasma following PCI (23), and it suggests the design of studies with therapies directed to binding and inactivating OxPL or other OSE released during percutaneous coronary, carotid, SVG, or peripheral interventions. For example, this could be achieved by infusing oxidation-specific antibodies or similarly directed therapies at time of presentation of an acute vascular syndrome or prior to intervention, such as with humanized E06-type antibodies or the human antibody IK17, which has been shown to bind OSE, prevent foam cell formation, and reduce atherosclerosis progression when infused in atherosclerotic mice (9). Because this study is retrospective and cross-sectional, it does not prove causality for the role of OSE in plaque progression and rupture. Future studies using human OSE antibodies therapeutically and showing clinical efficacy will be needed to prove the role of OSE in mediating CVD events.

REFERENCES

1. Miller, Y. I., S. H. Choi, P. Wiesner, L. Fang, R. Harkewicz, K. Hartvigsen, A. Boullier, A. Gonen, C. J. Diehl, X. Que, et al. 2011. Oxidation-specific epitopes are danger-associated molecular patterns recognized by pattern recognition receptors of innate immunity. *Circ. Res.* **108:** 235–248.
2. Chang, M. K., C. J. Binder, Y. I. Miller, G. Subbanagounder, G. J. Silverman, J. A. Berliner, and J. L. Witztum. 2004. Apoptotic cells with oxidation-specific epitopes are immunogenic and proinflammatory. *J. Exp. Med.* **200:** 1359–1370.
3. Briley-Saebo, K. C., P. X. Shaw, W. J. Mulder, S. H. Choi, E. Vucic, J. G. Aguinaldo, J. L. Witztum, V. Fuster, S. Tsimikas, and Z. A. Fayad. 2008. Targeted molecular probes for imaging atherosclerotic lesions with magnetic resonance using antibodies that recognize oxidation-specific epitopes. *Circulation.* **117:** 3206–3215.
4. Briley-Saebo, K. C., Y. S. Cho, P. X. Shaw, S. K. Ryu, V. Mani, S. Dickson, E. Izadmehr, S. Green, Z. A. Fayad, and S. Tsimikas. 2011. Targeted iron oxide particles for in vivo magnetic resonance detection of atherosclerotic lesions with antibodies directed to oxidation-specific epitopes. *J. Am. Coll. Cardiol.* **57:** 337–347.
5. Briley-Saebo, K. C., T. H. Nguyen, A. M. Saeboe, Y. S. Cho, S. K. Ryu, E. R. Volkova, S. Dickson, G. Leibundgut, P. Wiesner, S. Green, et al. 2012. In vivo detection of oxidation-specific epitopes

in atherosclerotic lesions using biocompatible manganese molecular magnetic imaging probes. *J. Am. Coll. Cardiol.* **59:** 616–626.
6. Aikawa, M., S. Sugiyama, C. C. Hill, S. J. Voglic, E. Rabkin, Y. Fukumoto, F. J. Schoen, J. L. Witztum, and P. Libby. 2002. Lipid lowering reduces oxidative stress and endothelial cell activation in rabbit atheroma. *Circulation.* **106:** 1390–1396.
7. Tsimikas, S., M. Aikawa, F. J. Miller, Jr., E. R. Miller, M. Torzewski, S. R. Lentz, C. Bergmark, D. D. Heistad, P. Libby, and J. L. Witztum. 2007. Increased plasma oxidized phospholipid:apolipoprotein B-100 ratio with concomitant depletion of oxidized phospholipids from atherosclerotic lesions after dietary lipid-lowering: a potential biomarker of early atherosclerosis regression. *Arterioscler. Thromb. Vasc. Biol.* **27:** 175–181.
8. Torzewski, M., P. X. Shaw, K. R. Han, B. Shortal, K. J. Lackner, J. L. Witztum, W. Palinski, and S. Tsimikas. 2004. Reduced in vivo aortic uptake of radiolabeled oxidation-specific antibodies reflects changes in plaque composition consistent with plaque stabilization. *Arterioscler. Thromb. Vasc. Biol.* **24:** 2307–2312.
9. Tsimikas, S., A. Miyanohara, K. Hartvigsen, E. Merki, P. X. Shaw, M. Y. Chou, J. Pattison, M. Torzewski, J. Sollors, T. Friedmann, et al. 2011. Human oxidation-specific antibodies reduce foam cell formation and atherosclerosis progression. *J. Am. Coll. Cardiol.* **58:** 1715–1727.
10. Taleb, A., J. L. Witztum, and S. Tsimikas. 2011. Oxidized phospholipids on apolipoprotein B-100 (OxPL/apoB) containing lipoproteins: a biomarker predicting cardiovascular disease and cardiovascular events. *Biomark. Med.* **5:** 673–694.
11. Schiopu, A., J. Bengtsson, I. Soderberg, S. Janciauskiene, S. Lindgren, M. P. S. Ares, P. K. Shah, R. Carlsson, J. Nilsson, and G. N. Fredrikson. 2004. Recombinant human antibodies against aldehyde-modified apolipoprotein B-100 peptide sequences inhibit atherosclerosis. *Circulation.* **110:** 2047–2052.
12. Caligiuri, G., J. Khallou-Laschet, M. Vandaele, A. T. Gaston, S. Delignat, C. Mandet, H. V. Kohler, S. V. Kaveri, and A. Nicoletti. 2007. Phosphorylcholine-targeting immunization reduces atherosclerosis. *J. Am. Coll. Cardiol.* **50:** 540–546.
13. Kramer, M. C., S. Z. Rittersma, R. J. de Winter, E. R. Ladich, D. R. Fowler, Y. H. Liang, R. Kutys, N. Carter-Monroe, F. D. Kolodgie, A. C. van der Wal, et al. 2010. Relationship of thrombus healing to underlying plaque morphology in sudden coronary death. *J. Am. Coll. Cardiol.* **55:** 122–132.
14. Farb, A., D. K. Weber, F. D. Kolodgie, A. P. Burke, and R. Virmani. 2002. Morphological predictors of restenosis after coronary stenting in humans. *Circulation.* **105:** 2974–2980.
15. Kolodgie, F. D., J. Narula, A. P. Burke, N. Haider, A. Farb, Y. Hui-Liang, J. Smialek, and R. Virmani. 2000. Localization of apoptotic macrophages at the site of plaque rupture in sudden coronary death. *Am. J. Pathol.* **157:** 1259–1268.
16. Virmani, R., F. D. Kolodgie, A. P. Burke, A. Farb, and S. M. Schwartz. 2000. Lessons from sudden coronary death: a comprehensive morphological classification scheme for atherosclerotic lesions. *Arterioscler. Thromb. Vasc. Biol.* **20:** 1262–1275.
17. Kolodgie, F. D., H. K. Gold, A. P. Burke, D. R. Fowler, H. S. Kruth, D. K. Weber, A. Farb, L. J. Guerrero, M. Hayase, R. Kutys, et al. 2003. Intraplaque hemorrhage and progression of coronary atheroma. *N. Engl. J. Med.* **349:** 2316–2325.
18. Young, S. G., J. L. Witztum, D. C. Casal, L. K. Curtiss, and S. Bernstein. 1986. Conservation of the low density lipoprotein receptor-binding domain of apoprotein B. Demonstration by a new monoclonal antibody, MB47. *Arteriosclerosis.* **6:** 178–188.
19. Boullier, A., P. Friedman, R. Harkewicz, K. Hartvigsen, S. R. Green, F. Almazan, E. A. Dennis, D. Steinberg, J. L. Witztum, and O. Quehenberger. 2005. Phosphocholine as a pattern recognition ligand for CD36. *J. Lipid Res.* **46:** 969–976.
20. Friedman, P., S. Horkko, D. Steinberg, J. L. Witztum, and E. A. Dennis. 2002. Correlation of antiphospholipid antibody recognition with the structure of synthetic oxidized phospholipids. Importance of Schiff base formation and aldol condensation. *J. Biol. Chem.* **277:** 7010–7020.
21. Tsimikas, S., W. Palinski, S. E. Halpern, D. W. Yeung, L. K. Curtiss, and J. L. Witztum. 1999. Radiolabeled MDA2, an oxidation-specific, monoclonal antibody, identifies native atherosclerotic lesions in vivo. *J. Nucl. Cardiol.* **6:** 41–53.
22. Shaw, P. X., S. Horkko, S. Tsimikas, M. K. Chang, W. Palinski, G. J. Silverman, P. P. Chen, and J. L. Witztum. 2001. Human-derived anti-oxidized LDL autoantibody blocks uptake of oxidized LDL by macrophages and localizes to atherosclerotic lesions in vivo. *Arterioscler. Thromb. Vasc. Biol.* **21:** 1333–1339.
23. Tsimikas, S., H. K. Lau, K. R. Han, B. Shortal, E. R. Miller, A. Segev, L. K. Curtiss, J. L. Witztum, and B. H. Strauss. 2004. Percutaneous coronary intervention results in acute increases in oxidized phospholipids and lipoprotein(a): short-term and long-term immunologic responses to oxidized low-density lipoprotein. *Circulation.* **109:** 3164–3170.
24. Seimon, T. A., M. J. Nadolski, X. Liao, J. Magallon, M. Nguyen, N. T. Feric, M. L. Koschinsky, R. Harkewicz, J. L. Witztum, S. Tsimikas, et al. 2010. Atherogenic lipids and lipoproteins trigger CD36–TLR2-dependent apoptosis in macrophages undergoing endoplasmic reticulum stress. *Cell Metab.* **12:** 467–482.
25. Berliner, J. A., N. Leitinger, and S. Tsimikas. 2009. The role of oxidized phospholipids in atherosclerosis. *J. Lipid Res.* **50(Suppl):** S207–S212.
26. Podrez, E. A., E. Poliakov, Z. Shen, R. Zhang, Y. Deng, M. Sun, P. J. Finton, L. Shan, M. Febbraio, D. P. Hajjar, et al. 2002. A novel family of atherogenic oxidized phospholipids promotes macrophage foam cell formation via the scavenger receptor CD36 and is enriched in atherosclerotic lesions. *J. Biol. Chem.* **277:** 38517–38523.
27. Shaw, P. X., S. Horkko, M. K. Chang, L. K. Curtiss, W. Palinski, G. J. Silverman, and J. L. Witztum. 2000. Natural antibodies with the T15 idiotype may act in atherosclerosis, apoptotic clearance, and protective immunity. *J. Clin. Invest.* **105:** 1731–1740.
28. Tsimikas, S., B. P. Shortal, J. L. Witztum, and W. Palinski. 2000. In vivo uptake of radiolabeled MDA2, an oxidation-specific monoclonal antibody, provides an accurate measure of atherosclerotic lesions rich in oxidized LDL and is highly sensitive to their regression. *Arterioscler. Thromb. Vasc. Biol.* **20:** 689–697.
29. Shao, B., S. Pennathur, I. Pagani, M. N. Oda, J. L. Witztum, J. F. Oram, and J. W. Heinecke. 2010. Modifying apolipoprotein A-I by malondialdehyde, but not by an array of other reactive carbonyls, blocks cholesterol efflux by the ABCA1 pathway. *J. Biol. Chem.* **285:** 18473–18484.
30. Tsimikas, S., Z. Mallat, P. J. Talmud, J. J. Kastelein, N. J. Wareham, M. S. Sandhu, E. R. Miller, J. Benessiano, A. Tedgui, J. L. Witztum, et al. 2010. Oxidation-specific biomarkers, lipoprotein(a), and risk of fatal and nonfatal coronary events. *J. Am. Coll. Cardiol.* **56:** 946–955.
31. Kiechl, S., J. Willeit, M. Mayr, B. Viehweider, M. Oberhollenzer, F. Kronenberg, C. J. Wiedermann, S. Oberthaler, Q. Xu, J. L. Witztum, et al. 2007. Oxidized phospholipids, lipoprotein(a), lipoprotein-associated phospholipase A2 activity, and 10-year cardiovascular outcomes: prospective results from the Bruneck study. *Arterioscler. Thromb. Vasc. Biol.* **27:** 1788–1795.
32. Bergmark, C., A. Dewan, A. Orsoni, E. Merki, E. R. Miller, M. J. Shin, C. J. Binder, S. Horkko, R. M. Krauss, M. J. Chapman, et al. 2008. A novel function of lipoprotein [a] as a preferential carrier of oxidized phospholipids in human plasma. *J. Lipid Res.* **49:** 2230–2239.
33. Rosenfeld, M. E., W. Palinski, S. Yla-Herttuala, S. Butler, and J. L. Witztum. 1990. Distribution of oxidation specific lipid-protein adducts and apolipoprotein B in atherosclerotic lesions of varying severity from WHHL rabbits. *Arteriosclerosis.* **10:** 336–349.
34. Scanlon, C. E. O., B. Berger, G. Malcom, and R. W. Wissler. 1996. Evidence for more extensive deposits of epitopes of oxidized low density lipoprotein in aortas of young people with elevated serum thiocyanate levels. *Atherosclerosis.* **121:** 23–33.
35. Weismann, D., K. Hartvigsen, N. Lauer, K. L. Bennett, H. P. Scholl, P. Charbel Issa, M. Cano, H. Brandstatter, S. Tsimikas, C. Skerka, et al. 2011. Complement factor H binds malondialdehyde epitopes and protects from oxidative stress. *Nature.* **478:** 76–81.
36. Ravandi, A., S. M. Boekholdt, Z. Mallat, P. J. Talmud, J. J. Kastelein, N. J. Wareham, E. R. Miller, J. Benessiano, A. Tedgui, J. L. Witztum, et al. 2011. Relationship of IgG and IgM autoantibodies and immune complexes to oxidized LDL with markers of oxidation and inflammation and cardiovascular events: results from the EPIC-Norfolk Study. *J. Lipid Res.* **52:** 1829–1836.
37. Tabas, I., K. J. Williams, and J. Boren. 2007. Subendothelial lipoprotein retention as the initiating process in atherosclerosis: update and therapeutic implications. *Circulation.* **116:** 1832–1844.
38. Lundstam, U., E. Hurt-Camejo, G. Olsson, P. Sartipy, G. Camejo, and O. Wiklund. 1999. Proteoglycans contribution to association of Lp(a) and LDL with smooth muscle cell extracellular matrix. *Arterioscler. Thromb. Vasc. Biol.* **19:** 1162–1167.

39. Dangas, G., J. A. Ambrose, D. J. D'Agate, J. H. Shao, S. Chockalingham, D. Levine, and D. A. Smith. 1999. Correlation of serum lipoprotein(a) with the angiographic and clinical presentation of coronary artery disease. *Am. J. Cardiol.* **83:** 583–585, A7.
40. Clarke, R., J. F. Peden, J. C. Hopewell, T. Kyriakou, A. Goel, S. C. Heath, S. Parish, S. Barlera, M. G. Franzosi, S. Rust, et al. 2009. Genetic variants associated with Lp(a) lipoprotein level and coronary disease. *N. Engl. J. Med.* **361:** 2518–2528.
41. Kamstrup, P. R., A. Tybjaerg-Hansen, R. Steffensen, and B. G. Nordestgaard. 2009. Genetically elevated lipoprotein(a) and increased risk of myocardial infarction. *JAMA.* **301:** 2331–2339.
42. Merki, E., M. J. Graham, A. E. Mullick, E. R. Miller, R. M. Crooke, R. E. Pitas, J. L. Witztum, and S. Tsimikas. 2008. Antisense oligonucleotide directed to human apolipoprotein B-100 reduces lipoprotein(a) levels and oxidized phospholipids on human apolipoprotein B-100 particles in lipoprotein(a) transgenic mice. *Circulation.* **118:** 743–753.
43. Cannon, C. P., S. Shah, H. M. Dansky, M. Davidson, E. A. Brinton, A. M. Gotto, M. Stepanavage, S. X. Liu, P. Gibbons, T. B. Ashraf, et al. 2010. Safety of anacetrapib in patients with or at high risk for coronary heart disease. *N. Engl. J. Med.* **363:** 2406–2415.
44. Raal, F. J., R. D. Santos, D. J. Blom, A. D. Marais, M. J. Charng, W. C. Cromwell, R. H. Lachmann, D. Gaudet, J. L. Tan, S. Chasan-Taber, et al. 2010. Mipomersen, an apolipoprotein B synthesis inhibitor, for lowering of LDL cholesterol concentrations in patients with homozygous familial hypercholesterolaemia: a randomised, double-blind, placebo-controlled trial. *Lancet.* **375:** 998–1006.